Downregulation of the Tem1 GTPase by Amn1 after cytokinesis involves both nuclear import and SCF-mediated degradation

Alain Devault, Simonetta Piatti

Downregulation of the Tem1 GTPase by Amn1 after cytokinesis involves both nuclear import and SCF-mediated degradation

Alain Devault and Simonetta Piatti*

CRBM, University of Montpellier, CNRS
1919 Route de Mende
34293 Montpellier (France)

*Corresponding author:
simonetta.piatti@crbm.cnrs.fr

ABSTRACT

At mitotic exit the cell cycle engine is reset to allow crucial processes, such as cytokinesis and replication origin licensing, to take place before a new cell cycle begins. In budding yeast, the cell cycle clock is reset by a Hippo-like kinase cascade called Mitotic Exit Network (MEN), whose activation is triggered at spindle pole bodies (SPBs) by the Tem1 GTPase. Yet, MEN activity must be extinguished once MEN-dependent processes have been accomplished. One factor contributing to switch off MEN is the Amn1 protein, which binds Tem1 and inhibits it through an unknown mechanism. Here, we show that Amn1 downregulates Tem1 through a dual mode. On one side, it evicts Tem1 from SPBs and escorts it into the nucleus. On the other, it promotes Tem1 degradation as part of an SCF ubiquitin ligase. Tem1 inhibition by Amn1 takes place after cytokinesis in the bud-derived daughter cell, consistent with its asymmetric appearance in the daughter versus the mother cell. This dual mechanism of Tem1 inhibition by Amn1 may contribute to rapidly extinguish MEN activity once it has fulfilled its functions.

INTRODUCTION

The Mitotic Exit Network (MEN) is an essential kinase cascade that promotes mitotic exit and cytokinesis in budding yeast (Bardin and Amon, 2001; Simanis, 2003). MEN has a similar organisation as the Septation Initiation Network in fission yeast and the Hippo pathway in metazoans, in that it includes a Ste20-like protein kinase (Cdc15) that activates a LATS-NDR kinase (Mob1-Dbf20/Df20) (Hergovich and Hemmings, 2012). A major function of MEN is to promote the release from the nucleolus and activate the Cdc14 phosphatase (Mohl et al., 2009; Shou et al., 1999; Visintin et al., 1999), i.e. the main CDK-counteracting phosphatase in budding yeast (Bouchoux and Uhlmann, 2011; Gray et al., 2003; Visintin et al., 1998).

MEN signalling is triggered by the Tem1 GTPase, which gets activated at microtubule-organizing centres or spindle pole bodies (SPBs) (reviewed in Scarfone and Piatti, 2015). During metaphase, Tem1 is present on both SPBs, albeit with a slight preference for the bud-proximal SPB. In anaphase it becomes markedly asymmetric, getting progressively concentrated on the bud-directed SPB (Bardin et al., 2000; Campbell et al., 2020; Caydasi and Pereira, 2009; Fraschini et al., 2006; Molk et al., 2004; Monje-Casas and Amon, 2009; Pereira et al., 2000; Scarfone et al., 2015). In spite of this asymmetry, both SPB-bound pools of Tem1 seem to contribute to mitotic exit (Campbell et al., 2020).
Once active, Tem1 recruits to SPBs and activates the MEN kinase Cdc15, which in turn phosphorylates the MEN scaffold Nud1, thereby creating a phospho-docking motif for the Mob1-Dbf2 kinase. At SPBs, Cdc15 activates Mob1-Dbf2 that ultimately allows Cdc14 nucleolar release and activation (Mah et al., 2001; Mohl et al., 2009; Rock and Amon, 2011; Rock et al., 2013; Scarfone et al., 2015; Valerio-Santiago and Monje-Casas, 2011; Visintin and Amon, 2001).

How MEN signalling is extinguished after cytokinesis is an important, yet unanswered, question. Indeed, unscheduled Cdc14 phosphatase activity in G1 interferes with DNA replication (Bloom and Cross, 2007). Furthermore, Cdc14-independent MEN functions (Hotz et al., 2012; Meitinger et al., 2011; Meitinger et al., 2013; Oh et al., 2012) might also need to be turned off.

One mechanism that contributes to MEN downregulation after mitotic exit is the re-entrapment of Cdc14 in the nucleolus prompted by Cdc14 itself (Lu and Cross, 2010; Manzoni et al., 2010; Visintin et al., 2008).

Another actor that contributes to turn down MEN signalling after mitotic exit is the MEN antagonist Amn1 protein. Amn1 is expressed from mitotic exit to late G1 and accumulates specifically in the nucleus of the bud-derived daughter cell (Wang et al., 2003). Asymmetric, cell cycle-dependent regulation of Amn1 expression requires the daughter-specific transcription factor Ace2 (Colman-Lerner et al., 2001) and Amn1 degradation in late G1 (Wang et al., 2003). In turn, Ace2 activation depends on MEN and Cdc14 (Brace et al., 2011; Sanchez-Diaz et al., 2012; Weiss et al., 2002). Thus, besides promoting its own re-entrapment, Cdc14 also triggers Amn1-dependent downregulation of MEN.

How exactly Amn1 antagonizes MEN signalling remains to be elucidated. Amn1 interacts physically with Tem1 and competes with Cdc15 for Tem1 binding (Wang et al., 2003). However, higher levels of Tem1 are present in *amn1⊿* cells (Wang et al., 2003), suggesting that Amn1 could inhibit Tem1 function also by promoting its turnover. Accordingly, in G1 Tem1 is present at low levels on SPBs (Campbell et al., 2020; Molk et al., 2004). Furthermore, Amn1 is an atypical F-box protein part of the SCF (Skp, Cullin, F-box-containing complex) ubiquitin ligase, driving proteolysis of Ace2 in most, but not all, laboratory strains (Fang et al., 2018).

Here, we show that Amn1 has a dual function in Tem1 downregulation after mitotic exit. On one side, it promotes Tem1 degradation as part of an SCF^{Amn1} complex, while on the other it displaces Tem1 from SPBs and escorts it into the nucleus independently of SCF.

RESULTS AND DISCUSSION

Amn1 prompts asymmetric removal of Tem1 from the daughter cell SPB and concomitant nuclear import after cytokinesis

To study Tem1 localisation, we used a strain expressing the endogenous *TEM1* gene tagged at the C-terminus with yeast-enhanced GFP (yeGFP). This strain has a doubling time indistinguishable from that of the isogenic untagged strain, suggesting that the tag does not perturb Tem1 activity (Fig. S1A). By live cell imaging, we observed a transient and asymmetric relocalisation of Tem1-yeGFP into the nucleus of the bud compartment, which was visualised by the nuclear marker mCherry-Pus1 (98/98 cells, Fig. 1A). Tem1 nuclear translocation occurred about 20 minutes after anaphase, and was accompanied by a decrease of Tem1 levels at the daughter-bound SPB. To better resolve the timing of Tem1 nuclear import, we filmed cells co-expressing Tem1-yeGFP and the mCherry-tagged septin Shs1. Tem1-yeGFP appeared in the nucleus of the bud 4 minutes (+/- 3 min; n=45) after septin ring disassembly, which marks the onset of cytokinesis (Lippincott et al., 2001; Tamborrini et al., 2018), and persisted in the nucleus throughout the following G1 phase until appearance of a new septin ring (Fig. S1B). Thus, Tem1 undergoes an asymmetric accumulation in the nucleus of the daughter cell after cytokinesis until late G1.

Next we investigated the molecular bases of Tem1 nuclear import. We reasoned that Amn1 could be implicated in this process since it interacts with Tem1 and is concentrated in the daughter cell nucleus after mitotic exit (Wang et al., 2003). In agreement with our prediction, Tem1-yeGFP nuclear import was completely abolished in *amn1Δ* cells (93/93 cells), and the protein persisted at both SPBs throughout the cell cycle (Fig. 1B). Furthermore, *AMN1* deletion increased the levels of Tem1 at the daughter cell SPB from cytokinesis to the following G1 without affecting Tem1 levels at the mother cell SPB (Fig. 1C).

Consistent with a role of Amn1 in downregulating Tem1 levels at SPBs specifically in G1, Tem1 levels were increased by more than twofold at SPBs of G1-arrested *amn1Δ* cells relative to their wild type counterparts (Fig. S1C).

Importantly, live cell imaging of cells co-expressing Amn1-sfGFP and Tem1-mScarlet-I showed that the two proteins concomitantly concentrate in the nucleus (104/109 cells, Fig. 1D).

These data suggest that Amn1 could escort Tem1 into the nucleus of the daughter cell to reduce its active pool at the daughter-bound SPB after cytokinesis, i.e. once Tem1 has accomplished its essential functions.

The SCF^{Amn1} complex promotes Tem1 ubiquitination and degradation

Amn1 is an atypical F-box protein that was recently shown to be part of an SCF (Skp, Cullin, F-box-containing) complex (Fang et al., 2018). In agreement with these data, we confirmed by co-immunoprecipitation experiments that Flag-tagged Amn1 (Amn1-3Flag) interacts with the HA-tagged cullin Cdc53 and Skp1 also in our strain background (W303, Fig. 2A-B, lane 3).

We then asked if Tem1 is associated with the SCF^{Amn1} complex. First, we confirmed the association between Tem1-3HA and Amn1-3Flag by co-immunoprecipitations (Fig. 2C, lane 2). Second, we asked if Cdc53-6HA could be co-immunoprecipitated with Tem1-3Flag from cells endogenously expressing both proteins. Results showed that indeed Tem1 binds to Cdc53 in wild type cells, while interaction is severely impaired in *amn1⊿* cells (Fig. 2D, lanes 2-3), suggesting that Tem1 binding to SCF is mediated by Amn1.

Tem1 interaction with SCF^{Amn1} suggests that Tem1 might be targeted to ubiquitin-mediated degradation and/or ubiquitin-dependent nuclear import. Therefore, we assessed if Tem1 ubiquitination (Cassani et al., 2013; Tamborrini et al., 2018) is regulated during the cell cycle and Amn1-dependent. To this end, we carried out Ni-NTA pulldowns of ubiquitinated proteins from synchronised cells overexpressing untagged or His-tagged ubiquitin, followed by western blot to detect Tem1-3HA. Since Amn1 is expressed after mitotic exit, cells were synchronised in late mitosis through the temperature-sensitive *cdc15-2* mutation and released at permissive temperature. Under these conditions, we could detect mono- and poly-ubiquitinated forms of Tem1, some of which were periodic during the cell cycle (Fig. 2E). Remarkably, cell cycle-regulated Tem1 ubiquitination peaked at 30 minutes after the late mitotic release, i.e. when Amn1-3Flag levels rose (Fig. 2E), and was drastically impaired by *AMN1* deletion, suggesting that it is greatly facilitated by Amn1, presumably bound to SCF.

Finally, we analysed the impact of Amn1-dependent ubiquitination on Tem1 turnover. To this end, *amn1⊿* and *GAL1-AMN1* cells carrying an extra copy of *TEM1* under the control of the *GAL1* promoter were synchronised in G1 and subjected to a short pulse (30') of galactose induction, followed by glucose-mediated repression. Tem1 decay was

accelerated by the pulse of Amn1 (Fig. 2F), suggesting that Tem1 ubiquitination by SCF^{Amn1} mildly stimulates Tem1 proteolysis. Consistently, *AMN1* deletion led to a two- to three-fold increase in Tem1 steady state levels (Fig. 3F), in agreement with a previous report (Wang et al., 2003).

Altogether, these data suggest that Tem1 interaction with and ubiquitination by SCF^{Amn1} from cytokinesis to late G1 stimulates Tem1 degradation.

A nuclear localization signal in Amn1, but not its F-box domain, mediates Tem1 nuclear translocation

To assess if Amn1-bound SCF is involved in Tem1 nuclear import, besides its proteolysis, we deleted the F-box domain of Amn1 (aa 166-263, Fig. 3A). Indeed, F-box motifs mediate the binding of F-box proteins to SCF (Bai et al., 1996). As expected, Amn1-ΔFbox no longer associated to Skp1 (Fig. 2B, lane 4). In addition, F-box deletion in Amn1 abolished the binding of Tem1 to Cdc53 without affecting Tem1-Amn1 interaction (Fig. 2C-D, lane 4). Thus, the F-box motif of Amn1 is necessary for Amn1 and Tem1 interaction with SCF, but not for Amn1 binding to Tem1. Interestingly, F-box deletion led to higher levels of Amn1-3Flag, as assessed by western blot (Fig. S2), consistent with the finding that Amn1 proteolysis in G1 requires SCF (Wang et al., 2003). It should be noticed, however, that Amn1-ΔFbox protein levels kept nevertheless oscillating during the cell cycle with similar kinetics to full length Amn1, suggesting that additional ubiquitin ligases control its degradation.

Live cell imaging of Tem1-GFP localisation in *amn1-ΔFbox* cells showed that Tem1 nuclear import was not affected (102/102 cells, Fig. 3B), while its levels at the daughter SPB in G1 were moderately increased (Fig. 3C). Therefore, Amn1 promotes Tem1 nuclear import independently of SCF.

We then wondered which could be the key determinants of Amn1 that mediate Tem1 nuclear import. Using the cNLS-Mapper prediction software (Kosugi et al., 2009), we found a putative bipartite nuclear localisation signal (NLS) in the primary sequence of Amn1 (aa 13-31, Fig. 3A). GFP-tagged Amn1 was readily detected in the nucleus of daughter cells after cytokinesis (59/60 cells, Fig. 3D left), as previously shown (Wang et al., 2003). Mutating pairs of basic residues in the NLS into alanine (aa 13-14 and 30-31), either together (Amn1-4A, Fig. 3D right) or separately (Amn1-$A_{13}A_{14}$ and Amn1-$A_{30}A_{31}$, Fig. S3), prevented Amn1nuclear translocation (55/56 *amn1-4A* cells; 1/56 cells with no

fluorescence), while the protein accumulated asymmetrically in the cytoplasm of the daughter cell. Thus, the identified NLS is crucial for Amn1 nuclear localisation. The lack of Amn1 diffusion between mother and bud compartment is consistent with the notion that Amn1 synthesis occurs after cytokinesis, i.e. after complete separation of mother and bud cytoplasm. Importantly, the *amn1-4A* mutant allele did neither affect Amn1 binding to Skp1 (Fig. 2B, lane 5) nor Tem1 interaction with Amn1 and Cdc53 (Fig. 2C, lane 3; Fig. 2D, lane 5).

In agreement with an escorting function of Amn1 in Tem1 nuclear import, Tem1 was not translocated into the nucleus of *amn1-4A* cells at any cell cycle stage (70/70 cells, Fig. 3E and S4). Moreover, Tem1 completely disappeared from the daughter cell SPB during G1 (i.e. around the time of cytoplasmic accumulation of Amn1, Fig. 3E and S4), indicating that binding to Amn1 evicts Tem1 from SPBs even in the absence of nuclear translocation. Remarkably, *amn1-4A* cells displayed even lower levels of Tem1 at the daughter SPB in G1 than wild type cells (Fig. 3C). This is likely a consequence of Amn1 failure to enter the nucleus, which increases its window of opportunity for dislodging Tem1 from the SPB.

We took advantage of the *amn1-4A* mutant to assess the possible contribution of Tem1 nuclear import on its proteolysis. By analysing Tem1 protein levels by western blot, we found that F-box deletion or NLS mutation individually caused a mild stabilization of Tem1 in G1, while deletion of both motifs together led to an additive increase in Tem1 levels, albeit not as pronounced as in *amn1Δ* cells (Fig. 3F). Conversely, *AMN1* overexpression from the galactose-inducible *GAL1* promoter (*GAL1-AMN1*) dramatically decreased Tem1 protein levels in an F-box-dependent manner (Fig. 3G). Thus, nuclear import and binding to SCF both contribute to Tem1 proteolysis.

In summary, Amn1 inhibits Tem1 at SPBs by two different mechanisms: SCF-mediated protein degradation and SCF-independent nuclear translocation (Fig. 4). Whether Tem1 has functions independent of MEN inside the nucleus is an intriguing possibility that deserves further investigation.

Given that Tem1 gets activated at SPBs, the dual mode of action of Amn1 may ensure rapid Tem1 inactivation after cytokinesis. Competition between Amn1 and Cdc15 for their association with Tem1 (Wang et al., 2003) could provide an additional mode of Tem1 downregulation.

Since *AMN1* expression requires the transcription factor Ace2, which in turn enters the nucleus upon MEN-dependent activation of Cdc14, Tem1 eviction from the daughter SPB and degradation are only possible after Tem1 has fulfilled its MEN-promoting functions. On the other hand, being Amn1 itself and Ace2 targets of SCF^{Amn1}, their clearance in G1 re-sets the stage for Tem1 re-accumulation in the following S and M phases. Thus, this sophisticated cell cycle circuit contributes to the ordered relay of MEN-regulated processes.

MATERIALS AND METHODS

Yeast strains, plasmids and growth conditions

All yeast strains (Table S1) are congenic to or at least four times backcrossed to W303 (*ade2-1, trp1-1, leu2-3,112, his3-11,15, ura3*).

One-step tagging techniques were used to generate 3HA-, yeGFP-, sfGFP, mScarlet-I and mCherry-tagged proteins at the C-terminus. The Tem1-yeGFP construct had been previously described (Scarfone et al., 2015). A Yiplac211 plasmid bearing *mCherry-PUS1* (gift from Maria Moriel Carretero) was integrated at the *ura3* locus after cutting with ApaI. The *shs1-GFP*-bearing BYP6904 plasmid was obtained from the National BioResource Project (Yeast) (https://yeast.nig.ac.jp/yeast) and used to generate the *shs1::LEU2::SHS1-GFP* strain after cutting with BglII and integration at the *SHS1* locus. *GAL1-TEM1* and *GAL1-AMN1* strains were generated by inserting a *natNT2-GAL1* cassette upstream the ATG at the *TEM1-3HA* and *AMN1-3Flag* locus, respectively. Since *TEM1* is an essential gene, the *natNT2-GAL1* cassette was integrated into a strain that carried an extra copy of *TEM1* on a centromeric plasmid. Strains deleted of the entire *AMN1* coding sequence were obtained by insertion of the *KanMX*, *K.l.URA3* or *C.a.URA3* cassettes by one-step transformation. A pRS313-*AMN1* plasmid (pSP1402) was constructed by inserting a DNA fragment covering the entire coding sequence of *AMN1* with 500 bp of 5' UTR and 178 bp of 3' UTR, amplified by PCR from genomic DNA of a wild type strain. Lys13 and Arg14 of Amn1 were both mutated to Ala by inserting a synthetic DNA duplex made of oligos MP902 and MP903 between the MluI and EcoRI sites in the *AMN1* gene. Lys30 and Lys31 of Amn1 were both mutated to Ala by inserting a synthetic DNA duplex carrying these mutations (Genecust) between the EcoRV and EcoRI sites in the *AMN1* gene. The deletion of the F-box domain of Amn1 (amino acids 163 to 263) was obtained by inverse PCR using oligos MP1037 and MP1038. Mutated *AMN1* alleles were transplaced at the *AMN1* locus by replacing the *URA3* marker in *amn1::K.l.URA3* or *amn1::C.a.URA3* strains followed by counter-selection on FoA-containing plates. The pRS413-*TEM1* plasmid (pSP526) contains the entire coding sequence for *TEM1* and 524 bp of 5' UTR.

Yeast cultures were grown at 25-30°C, in either SD medium (6.7 g/L yeast nitrogen base without aminoacids), supplemented with the appropriate nutrients, or YEP (1% yeast extract, 2% bactopeptone, 50 mg/L adenine) medium. Raffinose was supplemented to 2% (SD-raffinose or YEPR), glucose to 2% (SD-glucose or YEPD), and galactose to 1% (SD-raffinose/galactose or YEPRG). Cells were synchronized in G1 by alpha factor (4 µg/mL)

in YEP medium containing the appropriate sugar at 25°C. G1 arrest was monitored under a transmitted light microscope and cells were released in fresh medium (typically after 120–135 min of alpha factor treatment) at 30°C, unless otherwise specified, after being collected by centrifugation at 2000*g* followed by one wash with YEP containing the appropriate sugar.

Detection of ubiquitin conjugates

Analysis of 6His-tagged ubiquitin Tem1 conjugates was performed as previously described (Tamborrini et al., 2018).

FACS analysis of DNA contents

Yeast cells were collected and treated as described (Benzi et al., 2020) and analysed on a ACEA NovoCyte cytometer.

Protein extracts, immunoprecipitations and western blotting

For TCA protein extracts, 10–15 mL of cell culture in logarithmic phase (OD600 = 0.5-1) were collected by centrifugation at 2000*g*, washed with 1 mL of 20% TCA and resuspended in 100 µL of 20% TCA before breakage of cells with glass beads (diameter 0.5–0.75 mm) on a Vibrax VXR (IKA). After addition of 400 µL of 5% TCA, lysates were centrifuged for 10 min at 845*g*. Protein precipitates were resuspended in 100 µL of 3X SDS sample buffer (240 mM Tris-Cl pH6.8, 6% SDS, 30% glycerol, 2.28 M β-mercaptoethanol, 0.06% bromophenol blue), denatured at 99°C for 3 min and loaded on SDS-PAGE after elimination of cellular debris by centrifugation (5 min at 20000 *g*).

Native yeast protein extracts for immunoprecipitations were performed from cell pellets (equivalent to ~50 OD_{600}), after centrifugation at 2000*g* and washing with 1 mL of cold 10 mM Tris-Cl pH 7.5. Cells were then lysed using glass beads in a Bullet Blender in 25 mM Tris-Cl pH 7.4, 100 mM NaCl, 2 mM EDTA, 1 mM DTT, 0.1% IGEPAL containing a cocktail of protease inhibitors (Complete EDTA-free Roche) and phosphatase inhibitors (PhosSTOP Roche). Lysates were cleared at 20000*g* for 10 min at 4 °C and incubated on a nutator for 2h at 4 °C with 15 µL of protein-G Dynabeads and anti-Flag-M2 antibodies. After washing the beads three times, proteins were eluted in 50 mM Tris-HCl pH 8.3, 1 mM EDTA, 0.1% SDS containing 0.5 mg/ml of Flag peptide.

For western blotting, proteins were wet-transferred on Protran membranes (Schleicher and Schuell). Total proteins were revealed by amido-black staining and quantified with ImageJ after scanning the membranes. Specific proteins were detected with monoclonal anti-HA 12CA5 (AgroBio, 1:5000) or monoclonal anti-Flag M2 (Sigma F3165, 1:5000). Antibodies were diluted in 5% low-fat milk (Regilait) dissolved in TBST. Secondary antibodies were purchased from GE-Healthcare and proteins were detected by a luminol/p-coumaric acid enhanced chemiluminescence system. Membranes were imaged with a Amersham Imager-600 and protein bands were quantifies with ImageJ.

Fluorescence microscopy

Imaging of Tem1 at SPBs in cells arrested in G1 with alpha factor was performed after fixation in 4% PFA. Still digital images were taken with an oil immersion 100X 1.4 HCX PlanApochromat objective (Zeiss) with a Coolsnap-HQ2 CDD camera (Photometrics) mounted on a Zeiss AxioimagerZ1 fluorescence microscope and controlled by the MetaMorph imaging system software. Z stacks containing 18 planes were acquired with a step size of 0.3 µm and max-projected using ImageJ. Fluorescence intensities were measured with ImageJ. SPB particles were identified on the Spc42-mCherry images with the ImageJ Analyze Particles tool after applying a threshold. Maximum pixel values present in these SPB particles were extracted in both Spc42-mCherry and Tem1-yeGFP images. Background values for both channels were determined as the mean pixel value of several regions outside SPB particles. The $\log_2$ of Tem1 signals was finally plotted according to the following equation: $\log_2((SPB^{MAX} - Bkgnd)^{GFP}/(SPB^{MAX} - Bkgnd)^{mCherry})$ (Fig. S1B, 3C). For time-lapse video microscopy, cells were mounted on 0.8% agarose pads in SD medium on Fluorodishes and filmed at controlled temperature (30°C) with a 100X 1.49 NA oil immersion objective mounted on a Nikon Eclipse Ti microscope equipped with an EMCCD Evolve-512 Camera (Photometrics) and iLAS2 module (Roper Scientific) and controlled by Metamorph. Z stacks of 13 planes were acquired every 3-4 min with a step size of 0.4 µm in HILO mode. Z stacks were max-projected with ImageJ. Alternatively, time-lapse video microscopy was performed using a 100X Plan Apo lambda 1.45 NA objective mounted on a Dragonfly Andor spinning disk equipped with dual camera for 2-channel simultaneous acquisition and coupled to a Ti2 Nikon microscope (Fig 3C). Tem1 signals at SPBs were quantified as above, except that the background was calculated for each individual SPB as the mean pixel value in the vicinity of the SPB.

ACKNOWLEDGEMENTS

We are grateful to Maria Moriel-Carretero for the mCherry-*PUS1* plasmid, to Marco Geymonat and all members of Piatti's lab for useful discussions. We acknowledge the imaging core facility MRI, member of the national infrastructure France-BioImaging supported by the French National Research Agency (ANR-10-INBS-04, "Investments for the future").

COMPETING INTERESTS

No competing interests declared.

FUNDING

This work has been supported by the Fondation pour la Recherche Médicale (DEQ20150331740 to S.P.), Fondation ARC (PJA 20141201926 to S.P.) and Agence Nationale de la Recherche (ANR-18-CE13-0015-01 to S.P.).

REFERENCES

Bai, C., Sen, P., Hofmann, K., Ma, L., Goebl, M., Harper, J. W. and Elledge, S. J. (1996). SKP1 connects cell cycle regulators to the ubiquitin proteolysis machinery through a novel motif, the F-box. *Cell* **86**, 263–74.

Bardin, A. J. and Amon, A. (2001). Men and sin: what's the difference? *Nat Rev Mol Cell Biol* **2**, 815–26.

Bardin, A. J., Visintin, R. and Amon, A. (2000). A mechanism for coupling exit from mitosis to partitioning of the nucleus [In Process Citation]. *Cell* **102**, 21–31.

Benzi, G., Camasses, A., Atsunori, Y., Katou, Y., Shirahige, K. and Piatti, S. (2020). A common molecular mechanism underlies the role of Mps1 in chromosome biorientation and the spindle assembly checkpoint. *EMBO reports* **21**, e50257.

Bloom, J. and Cross, F. R. (2007). Novel role for cdc14 sequestration: cdc14 dephosphorylates factors that promote DNA replication. *Mol Cell Biol* **27**, 842–53.

Bouchoux, C. and Uhlmann, F. (2011). A Quantitative Model for Ordered Cdk Substrate Dephosphorylation during Mitotic Exit. *Cell* **147**, 803–814.

Brace, J., Hsu, J. and Weiss, E. L. (2011). Mitotic exit control of the Saccharomyces cerevisiae Ndr/LATS kinase Cbk1 regulates daughter cell separation after cytokinesis. *Molecular and cellular biology* **31**, 721–35.

Campbell, I. W., Zhou, X. and Amon, A. (2020). Spindle pole bodies function as signal amplifiers in the Mitotic Exit Network. *Molecular Biology of the Cell* **31**, 906–916.

Cassani, C., Raspelli, E., Santo, N., Chiroli, E., Lucchini, G. and Fraschini, R. (2013). Saccharomyces cerevisiae Dma proteins participate in cytokinesis by controlling two different pathways. *Cell Cycle* **12**, 2794–808.

Caydasi, A. K. and Pereira, G. (2009). Spindle alignment regulates the dynamic association of checkpoint proteins with yeast spindle pole bodies. *Dev Cell* **16**, 146–56.

Colman-Lerner, A., Chin, T. E. and Brent, R. (2001). Yeast Cbk1 and Mob2 activate daughter-specific genetic programs to induce asymmetric cell fates. *Cell* **107**, 739–50.

Fang, O., Hu, X., Wang, L., Jiang, N., Yang, J., Li, B. and Luo, Z. (2018). Amn1 governs post-mitotic cell separation in Saccharomyces cerevisiae. *PLoS Genet.* **14**, e1007691.

Fraschini, R., D'Ambrosio, C., Venturetti, M., Lucchini, G. and Piatti, S. (2006). Disappearance of the budding yeast Bub2-Bfa1 complex from the mother-bound spindle pole contributes to mitotic exit. *J Cell Biol* **172**, 335–46.

Gray, C. H., Good, V. M., Tonks, N. K. and Barford, D. (2003). The structure of the cell cycle protein Cdc14 reveals a proline-directed protein phosphatase. *Embo J* **22**, 3524–

35.

Hergovich, A. and Hemmings, B. A. (2012). Hippo signalling in the G2/M cell cycle phase: lessons learned from the yeast MEN and SIN pathways. *Semin Cell Dev Biol* **23**, 794–802.

Hotz, M., Leisner, C., Chen, D., Manatschal, C., Wegleiter, T., Ouellet, J., Lindstrom, D., Gottschling, D. E., Vogel, J. and Barral, Y. (2012). Spindle pole bodies exploit the mitotic exit network in metaphase to drive their age-dependent segregation. *Cell* **148**, 958–72.

Kosugi, S., Hasebe, M., Tomita, M. and Yanagawa, H. (2009). Systematic identification of cell cycle-dependent yeast nucleocytoplasmic shuttling proteins by prediction of composite motifs. *PNAS* **106**, 10171–10176.

Lippincott, J., Shannon, K. B., Shou, W., Deshaies, R. J. and Li, R. (2001). The Tem1 small GTPase controls actomyosin and septin dynamics during cytokinesis. *J Cell Sci* **114**, 1379–86.

Lu, Y. and Cross, F. R. (2010). Periodic Cyclin-Cdk Activity Entrains an Autonomous Cdc14 Release Oscillator. *Cell* **141**, 268–279.

Mah, A. S., Jang, J. and Deshaies, R. J. (2001). Protein kinase Cdc15 activates the Dbf2-Mob1 kinase complex. *Proc Natl Acad Sci U S A* **98**, 7325–30.

Manzoni, R., Montani, F., Visintin, C., Caudron, F., Ciliberto, A. and Visintin, R. (2010). Oscillations in Cdc14 release and sequestration reveal a circuit underlying mitotic exit. *Journal of Cell Biology* **190**, 209–222.

Meitinger, F., Boehm, M. E., Hofmann, A., Hub, B., Zentgraf, H., Lehmann, W. D. and Pereira, G. (2011). Phosphorylation-dependent regulation of the F-BAR protein Hof1 during cytokinesis. *Genes Dev* **25**, 875–88.

Meitinger, F., Palani, S., Hub, B. and Pereira, G. (2013). Dual function of the NDR-kinase Dbf2 in the regulation of the F-BAR protein Hof1 during cytokinesis. *Mol Biol Cell* **24**, 1290–304.

Mohl, D. A., Huddleston, M. J., Collingwood, T. S., Annan, R. S. and Deshaies, R. J. (2009). Dbf2-Mob1 drives relocalization of protein phosphatase Cdc14 to the cytoplasm during exit from mitosis. *J Cell Biol*.

Molk, J. N., Schuyler, S. C., Liu, J. Y., Evans, J. G., Salmon, E. D., Pellman, D. and Bloom, K. (2004). The differential roles of budding yeast Tem1p, Cdc15p, and Bub2p protein dynamics in mitotic exit. *Mol Biol Cell* **15**, 1519–32.

Monje-Casas, F. and Amon, A. (2009). Cell polarity determinants establish asymmetry in

MEN signaling. *Dev Cell* **16**, 132–45.

Oh, Y., Chang, K. J., Orlean, P., Wloka, C., Deshaies, R. and Bi, E. (2012). Mitotic exit kinase Dbf2 directly phosphorylates chitin synthase Chs2 to regulate cytokinesis in budding yeast. *Molecular biology of the cell* **23**, 2445–56.

Pereira, G., Hofken, T., Grindlay, J., Manson, C. and Schiebel, E. (2000). The Bub2p spindle checkpoint links nuclear migration with mitotic exit. *Mol Cell* **6**, 1–10.

Piatti, S., Bohm, T., Cocker, J. H., Diffley, J. F. and Nasmyth, K. (1996). Activation of S-phase-promoting CDKs in late G1 defines a “point of no return” after which Cdc6 synthesis cannot promote DNA replication in yeast. *Genes Dev* **10**, 1516–31.

Rock, J. M. and Amon, A. (2011). Cdc15 integrates Tem1 GTPase-mediated spatial signals with Polo kinase-mediated temporal cues to activate mitotic exit. *Genes & development* **25**, 1943–54.

Rock, J. M., Lim, D., Stach, L., Ogrodowicz, R. W., Keck, J. M., Jones, M. H., Wong, C. C., Yates, J. R., 3rd, Winey, M., Smerdon, S. J., et al. (2013). Activation of the Yeast Hippo Pathway by Phosphorylation-Dependent Assembly of Signaling Complexes. *Science* **340**, 871–875.

Sanchez-Diaz, A., Nkosi, P. J., Murray, S. and Labib, K. (2012). The Mitotic Exit Network and Cdc14 phosphatase initiate cytokinesis by counteracting CDK phosphorylations and blocking polarised growth. *The EMBO journal* **31**, 3620–34.

Scarfone, I. and Piatti, S. (2015). Coupling spindle position with mitotic exit in budding yeast: The multifaceted role of the small GTPase Tem1. *Small GTPases* **6**, 1–6.

Scarfone, I., Venturetti, M., Hotz, M., Lengefeld, J., Barral, Y. and Piatti, S. (2015). Asymmetry of the budding yeast Tem1 GTPase at spindle poles is required for spindle positioning but not for mitotic exit. *PLoS genetics* **11**, e1004938.

Shou, W., Seol, J. H., Shevchenko, A., Baskerville, C., Moazed, D., Chen, Z. W., Jang, J., Charbonneau, H. and Deshaies, R. J. (1999). Exit from mitosis is triggered by Tem1-dependent release of the protein phosphatase Cdc14 from nucleolar RENT complex. *Cell* **97**, 233–44.

Simanis, V. (2003). Events at the end of mitosis in the budding and fission yeasts. *J Cell Sci* **116**, 4263–75.

Tamborrini, D., Juanes, M. A., Ibanes, S., Rancati, G. and Piatti, S. (2018). Recruitment of the mitotic exit network to yeast centrosomes couples septin displacement to actomyosin constriction. *Nat Commun* **9**, 4308.

Valerio-Santiago, M. and Monje-Casas, F. (2011). Tem1 localization to the spindle pole

bodies is essential for mitotic exit and impairs spindle checkpoint function. *J Cell Biol* **192**, 599–614.

Visintin, R. and Amon, A. (2001). Regulation of the mitotic exit protein kinases cdc15 and dbf2. *Mol Biol Cell* **12**, 2961–74.

Visintin, R., Craig, K., Hwang, E. S., Prinz, S., Tyers, M. and Amon, A. (1998). The phosphatase Cdc14 triggers mitotic exit by reversal of Cdk- dependent phosphorylation. *Mol Cell* **2**, 709–18.

Visintin, R., Hwang, E. S. and Amon, A. (1999). Cfi1 prevents premature exit from mitosis by anchoring Cdc14 phosphatase in the nucleolus [see comments]. *Nature* **398**, 818–23.

Visintin, C., Tomson, B. N., Rahal, R., Paulson, J., Cohen, M., Taunton, J., Amon, A. and Visintin, R. (2008). APC/C-Cdh1-mediated degradation of the Polo kinase Cdc5 promotes the return of Cdc14 into the nucleolus. *Genes Dev* **22**, 79–90.

Wang, Y., Shirogane, T., Liu, D., Harper, J. W. and Elledge, S. J. (2003). Exit from exit: resetting the cell cycle through Amn1 inhibition of G protein signaling. *Cell* **112**, 697–709.

Weiss, E. L., Kurischko, C., Zhang, C., Shokat, K., Drubin, D. G. and Luca, F. C. (2002). The Saccharomyces cerevisiae Mob2p-Cbk1p kinase complex promotes polarized growth and acts with the mitotic exit network to facilitate daughter cell-specific localization of Ace2p transcription factor. *J Cell Biol* **158**, 885–900.

Willems, A. R., Schwab, M. and Tyers, M. (2004). A hitchhiker's guide to the cullin ubiquitin ligases: SCF and its kin. *Biochimica et Biophysica Acta (BBA) - Molecular Cell Research* **1695**, 133–170.

FIGURE LEGENDS

Figure 1. Amn1 escorts Tem1 into the nucleus at the M/G1 transition.
A. Cells expressing Tem1-yeGFP and mCherry-Pus1 were imaged every 4 minutes. Arrows indicate nuclear Tem1. Tem1-yeGFP nuclear signals (mean ± s.d.) were plotted (graph) relative to the onset of anaphase (t=0; n=24). **B.** *Δamn1* cells expressing Tem1-yeGFP were imaged as in A. **C.** Wild type (wt) and *Δamn1* cells co-expressing Tem1-yeGFP, Shs1-GFP and Spc42-mCherry (SPB marker) were imaged every 3 minutes. Arrows indicate nuclear Tem1. Mean values (curves) and s.d. (shades) of Tem1-yeGFP signals normalised to Spc42-mcherry were plotted (graphs) relative to septin disassembly (t=0; n= 28-54). A.U.: Arbitrary units. **D.** Cells co-expressing Amn1-sfGFP and Tem1-mScarlet-I were imaged as in A. Arrows indicate Amn1 and Tem1 nuclear entry. DIC: Differential Interference Contrast. Scale bars: 5 µm. m: mother cell; d: daughter cell.

Figure 2. SCF^{Amn1} promotes Tem1 ubiquitination and degradation.
A-D. Amn1-3Flag (A,B,C), its mutant variants (ΔFbox, 4A) (B,C) or Tem1-3Flag (D) were immunoprecipitated from asynchronously growing cells. Immunoprecipitates (IP-Flag) were probed with an anti-HA antibody to detect Cdc53-6HA (A,D), Skp1-6HA (B) or Tem1-3HA (C). Note that Tem1-3HA reproducibly runs as a doublet (see also Fig. 2E-F, 3F-G).
E. *cdc15-2* temperature-sensitive cells overexpressing untagged or 6His-tagged ubiquitin were grown at 25°C (async) and shifted to 37°C for 3 hours (late mitotic arrest). After release in fresh medium at 25°C, cells were collected at the indicated times for Ni-NTA pulldowns of ubiquitinated proteins (His-PD) and FACS analysis of DNA contents (righthand histograms). Presence of ubiquitinated Tem1-3HA was assessed with an anti-HA antibody. Wild type cells co-expressed Amn1-3Flag to correlate Tem1 ubiquitination with Amn1 levels throughout the experiment. The experiment was repeated three times with similar results. Note that the bulk of DNA replication occurs at 45 minutes after release (righthand histograms; 1C: pre-replicative DNA content; 2C: post-replicative DNA content). The appearance of a 4C post-replicative peak of DNA content is due to the cell separation defect of *cdc15-2* cells (Piatti et al., 1996). **F.** *Δamn1* and *GAL1-AMN1* cells bearing an extra copy of 3HA-tagged *TEM1* under the control of the *GAL1* promoter, were grown in YEPR and synchronised in G1 with alpha factor. After 30 minutes induction with 1% galactose, cells were transferred to glucose-containing medium to switch off the *GAL1* promoter (*GAL1-AMN1* and *GAL1-TEM1-3HA*). Protein levels of Tem1-3HA (upper and

lower band) were quantified by western blot and normalised to the total protein levels in the samples (amido-Black staining) for plotting (graph). The experiment was repeated three times with similar results. A.U.: Arbitrary units. WCE: whole cell extracts.

Figure 3. The NLS of Amn1, but not its F-box domain, is required for Tem1 nuclear import.

A. Aminoacid sequence of Amn1 Fbox domain (Willems et al., 2004) and NLS (Kosugi et al., 2009). Conserved residues are highlighted in blue and red, respectively. **B.** Tem1-yeGFP was imaged every 4' in *amn1-ΔFbox* cells. Yellow arrows: SPB-localised Tem1-yeGFP; magenta arrows: nuclear Tem1-yeGFP. **C.** Live cells co-expressing Tem1-yeGFP, Shs1-GFP (septin) and Spc42-mCherry were imaged every 3 minutes. Tem1-yeGFP signals were quantified at the bud SPB 12' after mitotic exit, as assessed by disassembly of Shs1-GFP at the bud neck, and normalised relative to Spc42-mCherry. Medians, first and third quartiles are shown in red. *p*-values were obtained using a Mann-Whitney test. **D.** Amn1-yeGFP and Amn1-4A-yeGFP were imaged every 4'. Arrows indicate nuclear Amn1. **E.** Tem1-yeGFP and Spc42-mCherry were imaged every 4' in *amn1-4A* cells. Note the decrease of Tem1-yeGFP fluorescence at the bud SPB (times 16'-48'), in the absence of nuclear import. **F-G.** Protein levels of Tem1-3HA (upper and lower band) were quantified by western blot in total extracts from G1-arrested cells (F) or from asynchronously growing cells after overnight galactose induction (G). Protein levels were plotted (graph) relative to total protein levels (Coomassie staining). A.U. Arbitrary Units. N=3-5. Error bars: SD. DIC: Differential Interference Contrast. Scale bars: 5 μm. m: mother cell; d: daughter cell.

Figure 4. Dual mode of Tem1 regulation by Amn1.

Tem1 is active at SPBs, where it recruits and activates MEN (not depicted). Amn1 evicts Tem1 from the bud SPB through direct binding (1) and escorts it into the nucleus (2). Tem1 also associates with SCF^{Amn1}, presumably in the nucleus and in the cytoplasm, which leads to its degradation (3).

A

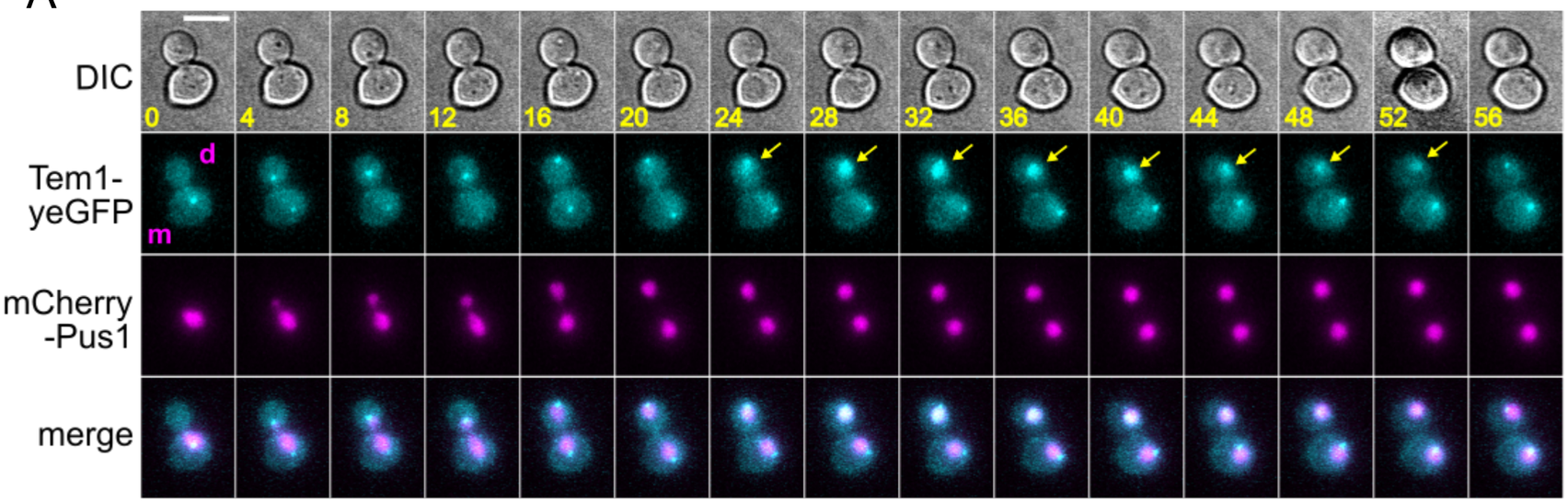
DIC
Tem1-yeGFP
mCherry-Pus1
merge
0
4
8
12
16
20
24
28
32
36
40
44
48
52
56
d
m

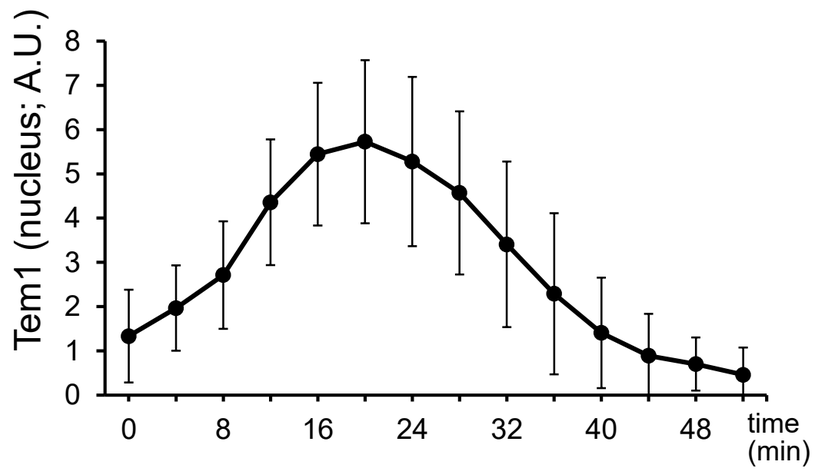
Tem1 (nucleus; A.U.)
time (min)
0
1
2
3
4
5
6
7
8
0
8
16
24
32
40
48

B

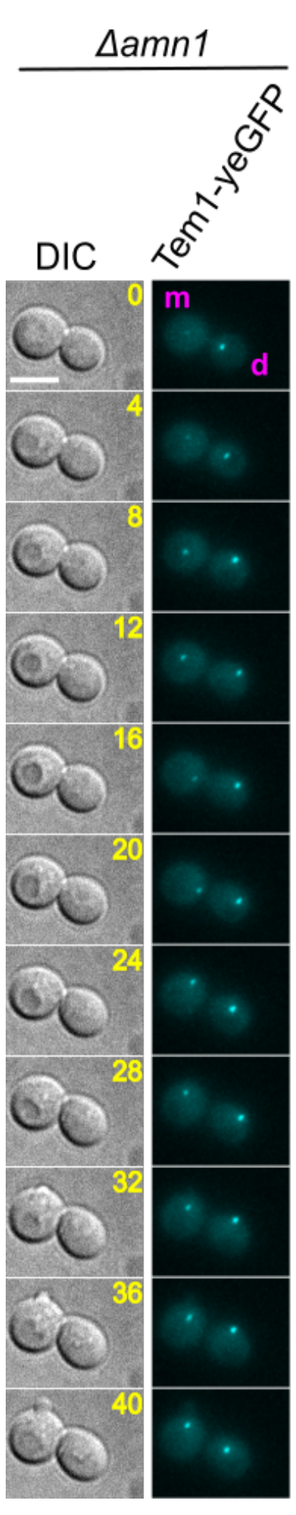
Δamn1
Tem1-yeGFP
DIC
0
4
8
12
16
20
24
28
32
36
40
m
d

C

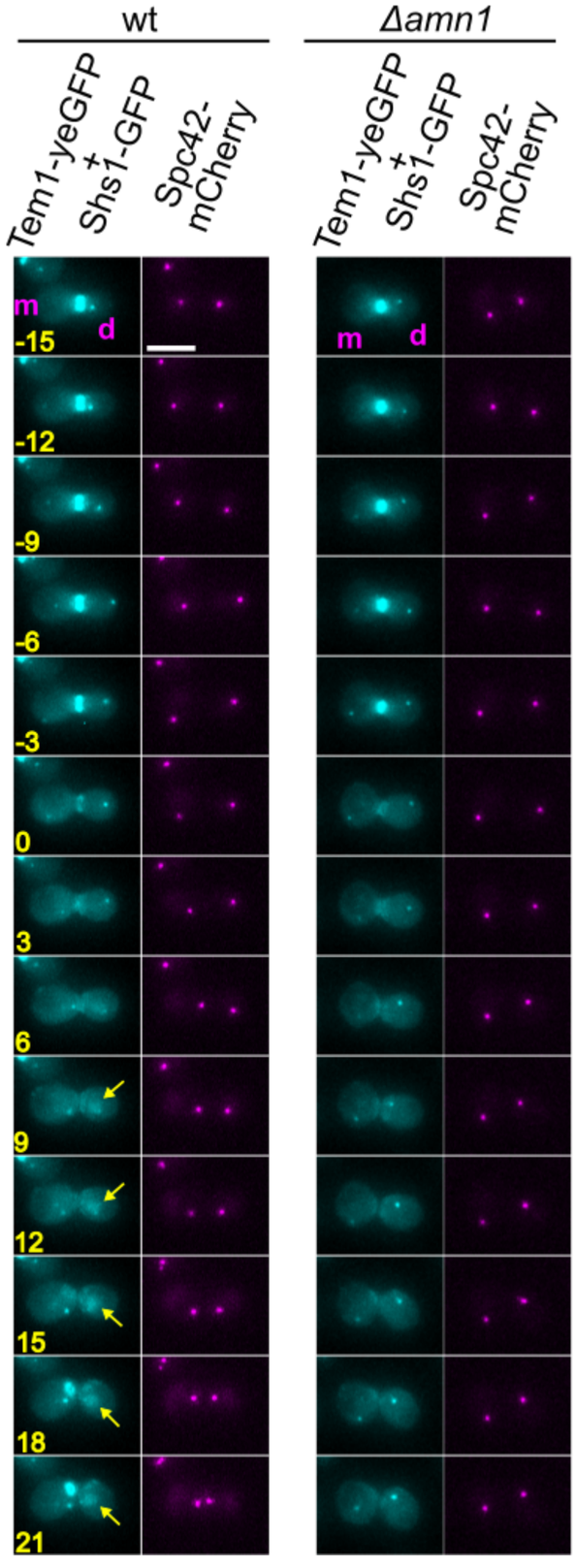
wt
Δamn1
Tem1-yeGFP + Shs1-GFP
Spc42-mCherry
-15
-12
-9
-6
-3
0
3
6
9
12
15
18
21
m
d

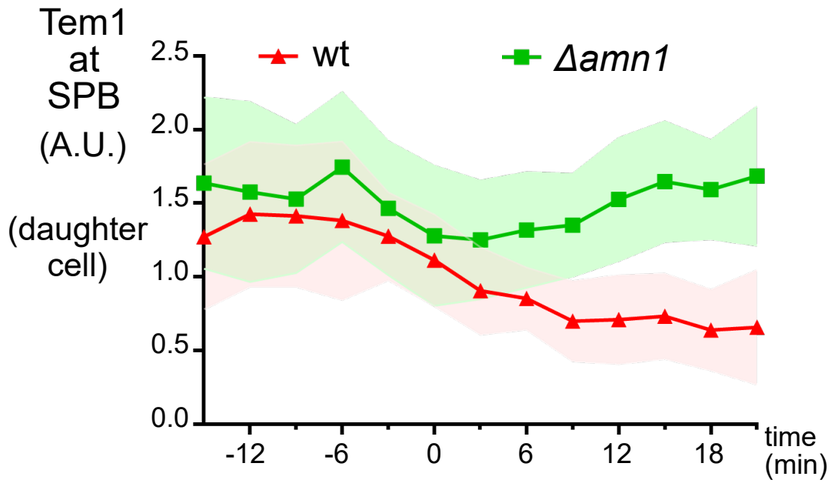
Tem1 at SPB (A.U.)
(daughter cell)
wt
Δamn1
time (min)
0.0
0.5
1.0
1.5
2.0
2.5
-12
-6
0
6
12
18

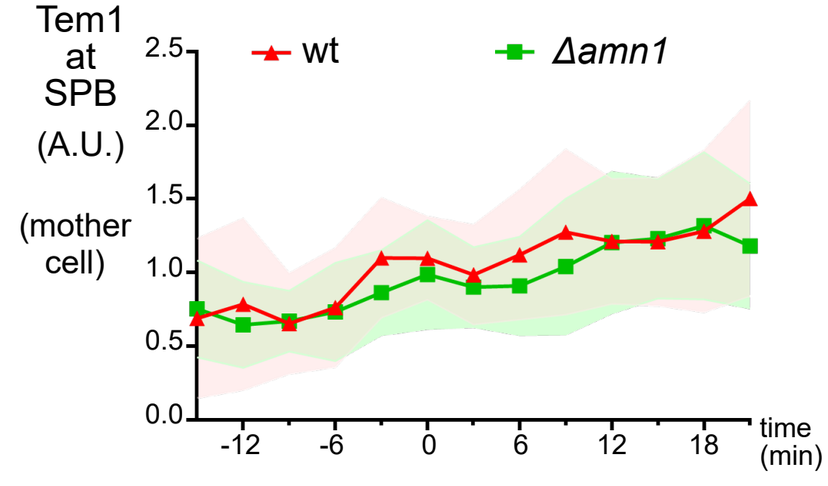
Tem1 at SPB (A.U.)
(mother cell)
wt
Δamn1
time (min)
0.0
0.5
1.0
1.5
2.0
2.5
-12
-6
0
6
12
18

D

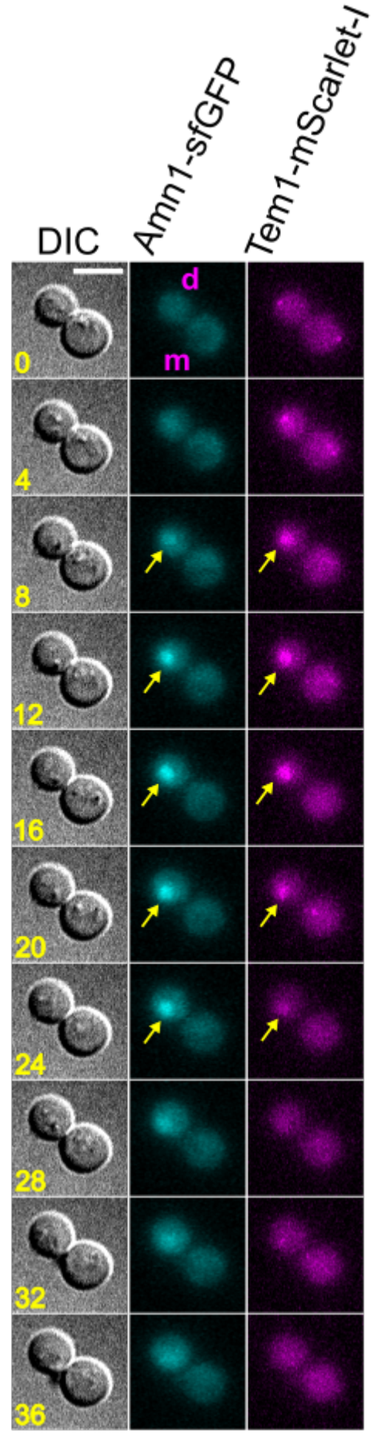
DIC
Amn1-sfGFP
Tem1-mScarlet-I
0
4
8
12
16
20
24
28
32
36
d
m

A

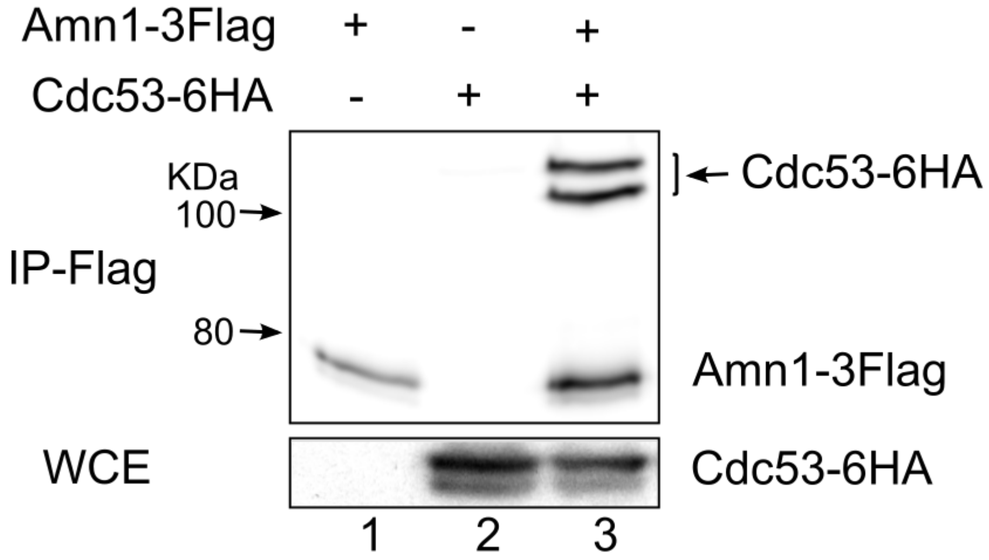
Amn1-3Flag + - +
Cdc53-6HA - + +
KDa
100
80
IP-Flag
Cdc53-6HA
Amn1-3Flag
WCE
Cdc53-6HA
1 2 3

B

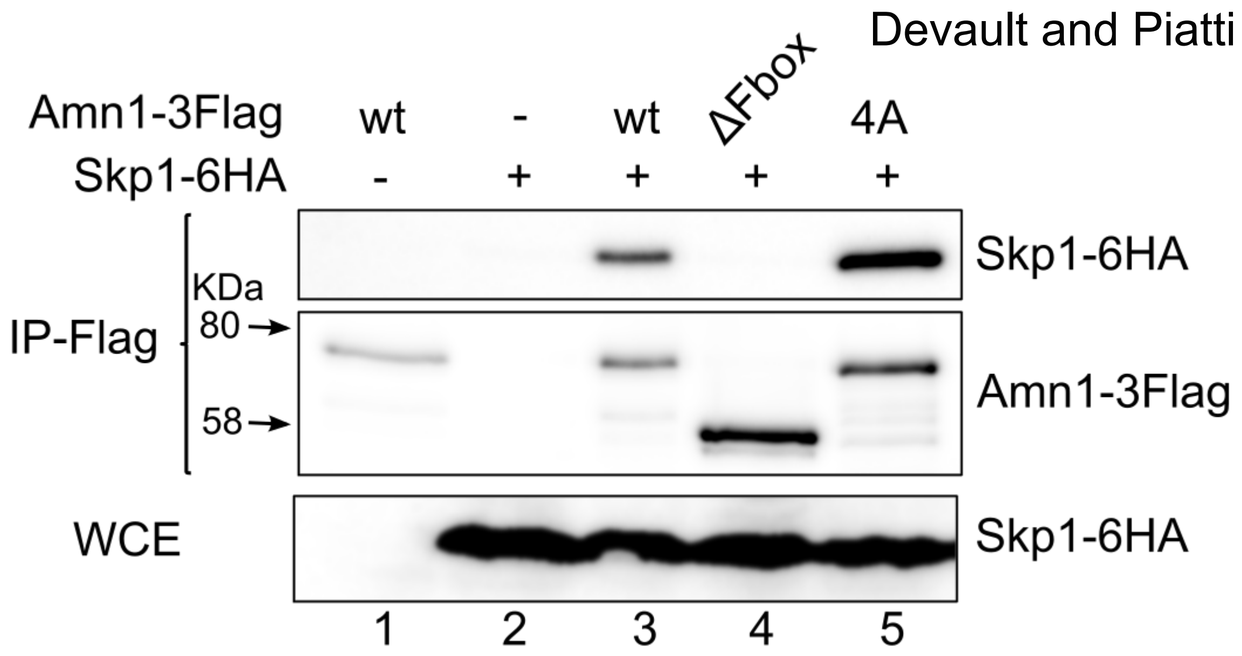
Amn1-3Flag wt - wt ΔFbox 4A
Skp1-6HA - + + + +
KDa
80
58
IP-Flag
Skp1-6HA
Amn1-3Flag
WCE
Skp1-6HA
1 2 3 4 5

C

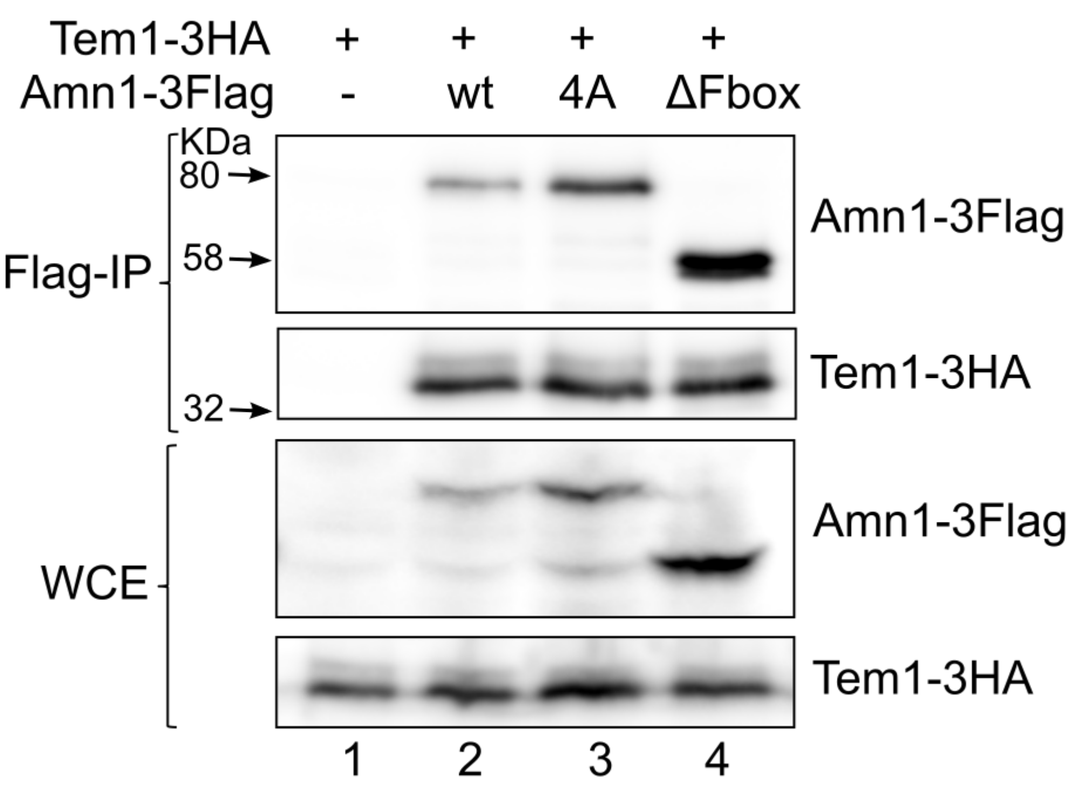
Tem1-3HA + + + +
Amn1-3Flag - wt 4A ΔFbox
KDa
80
58
32
Flag-IP
Amn1-3Flag
Tem1-3HA
WCE
Amn1-3Flag
Tem1-3HA
1 2 3 4

D

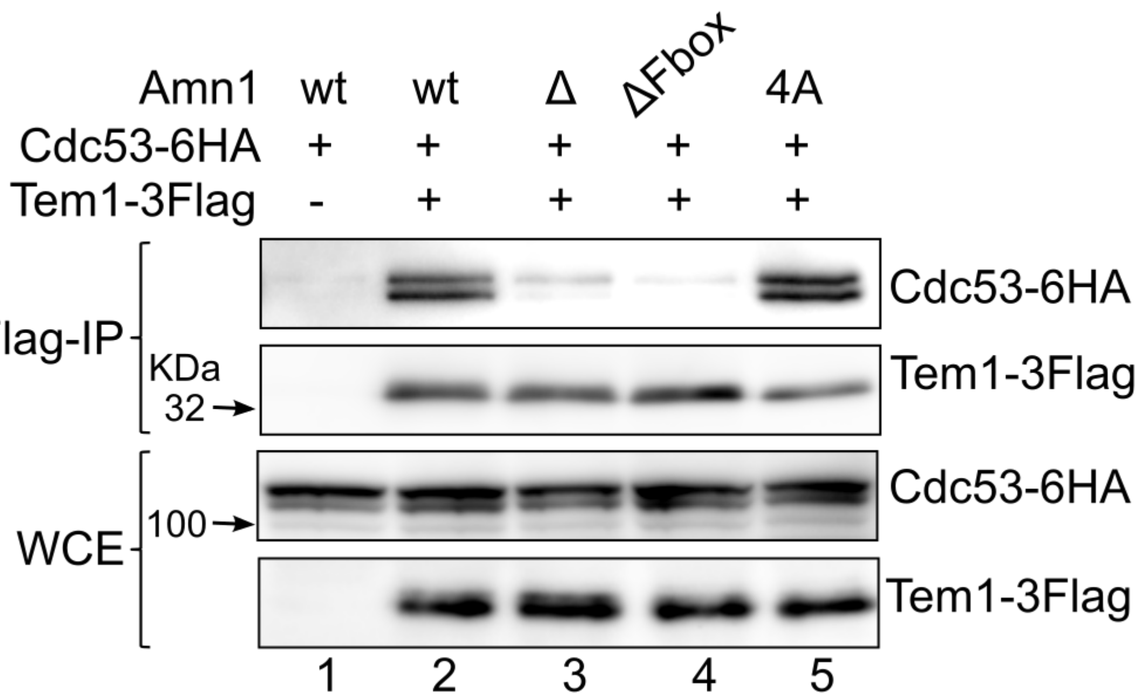
Amn1 wt wt Δ ΔFbox 4A
Cdc53-6HA + + + + +
Tem1-3Flag - + + + +
Flag-IP
KDa
32
Cdc53-6HA
Tem1-3Flag
WCE
100
Cdc53-6HA
Tem1-3Flag
1 2 3 4 5

E

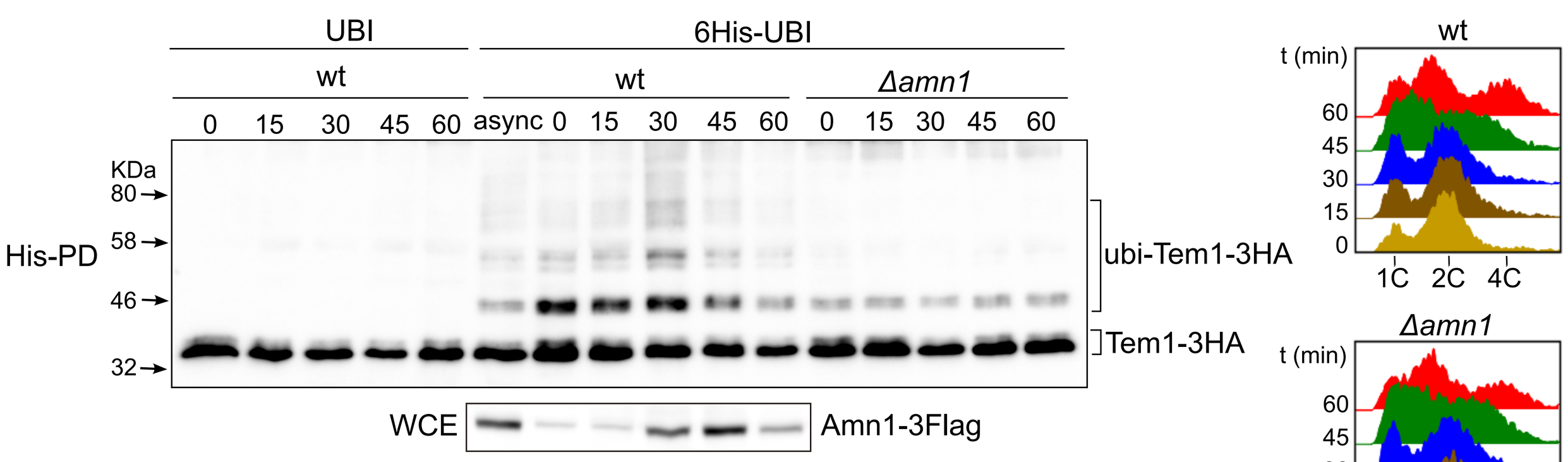
UBI
6His-UBI
wt
wt
Δamn1
0 15 30 45 60 async 0 15 30 45 60 0 15 30 45 60
KDa
80
58
46
32
His-PD
ubi-Tem1-3HA
Tem1-3HA
WCE
Amn1-3Flag
wt
t (min)
60
45
30
15
0
1C 2C 4C
Δamn1
t (min)
60
45
30
15
0
1C 2C 4C

F

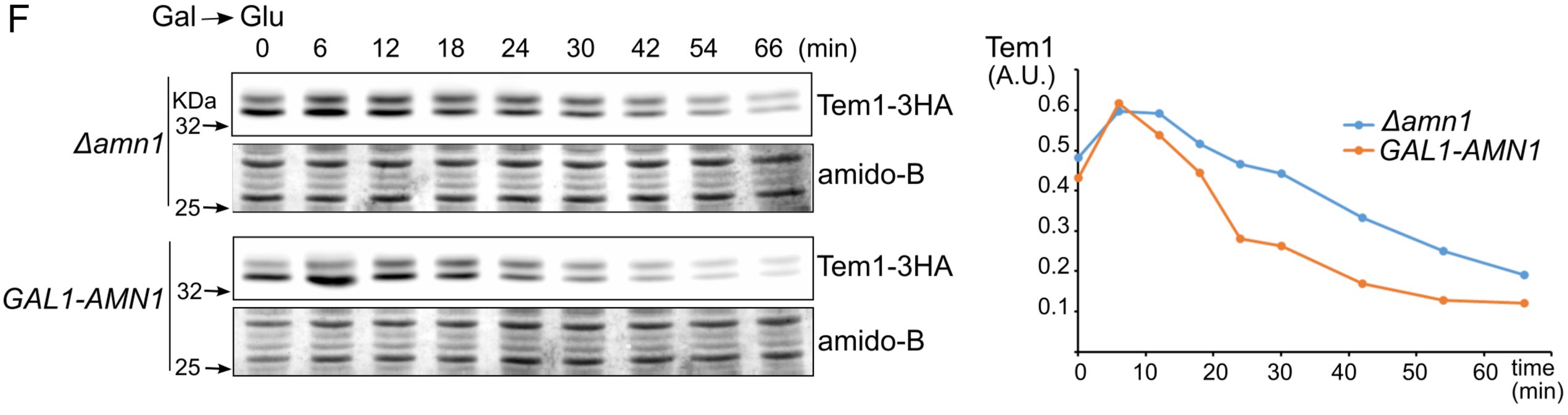
Gal → Glu
0 6 12 18 24 30 42 54 66 (min)
KDa
32
25
Δamn1
Tem1-3HA
amido-B
GAL1-AMN1
Tem1-3HA
amido-B
Tem1
(A.U.)
0.6
0.5
0.4
0.3
0.2
0.1
0 10 20 30 40 50 60
time
(min)
Δamn1
GAL1-AMN1

A

Fbox : 166 VFEIPEIVENIIKMIVSLES……(56)……LFSCMMVNRLWLNVTRPFLFKSLH 263

NLS : 1 MKLERVSSNGSFKRGRDIQSLESPCTRPLKKMSPSPSFTSL 40

B

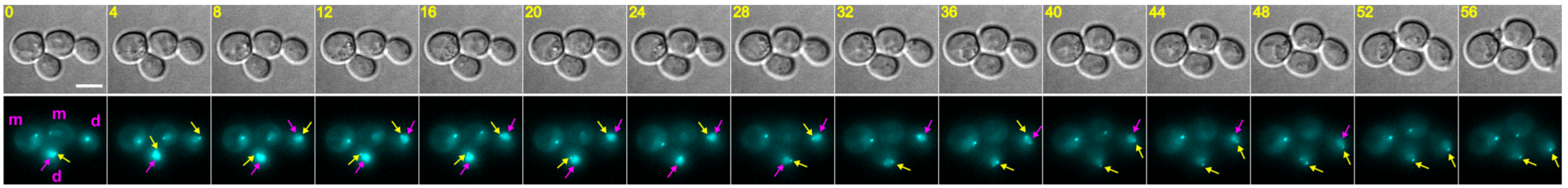

C

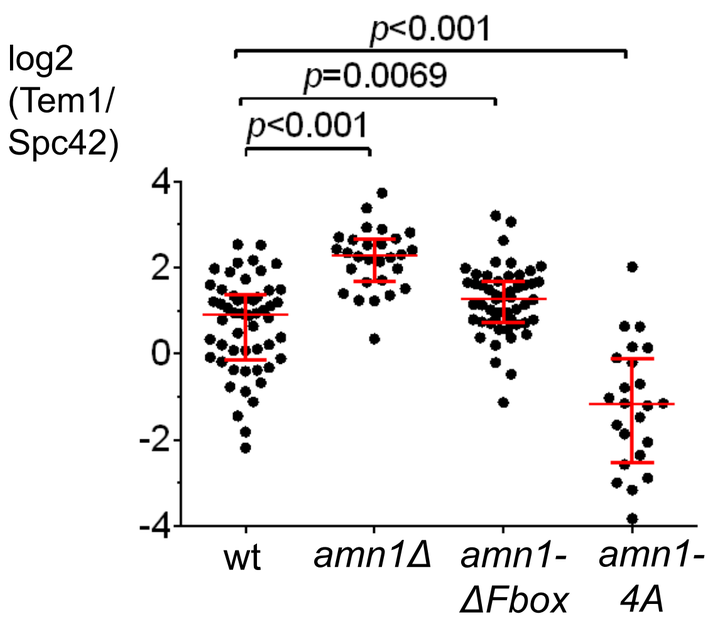

D

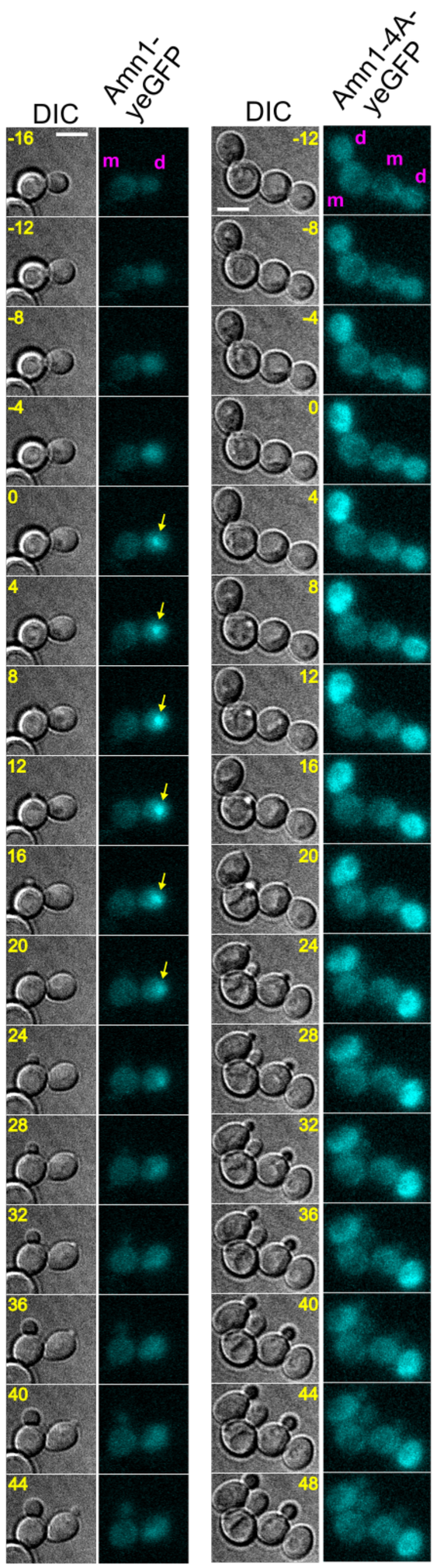

E

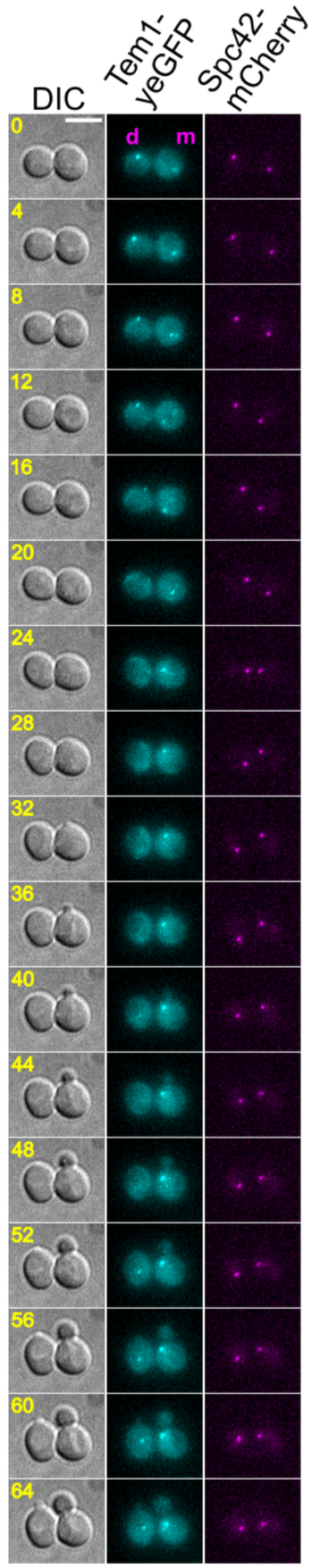

F

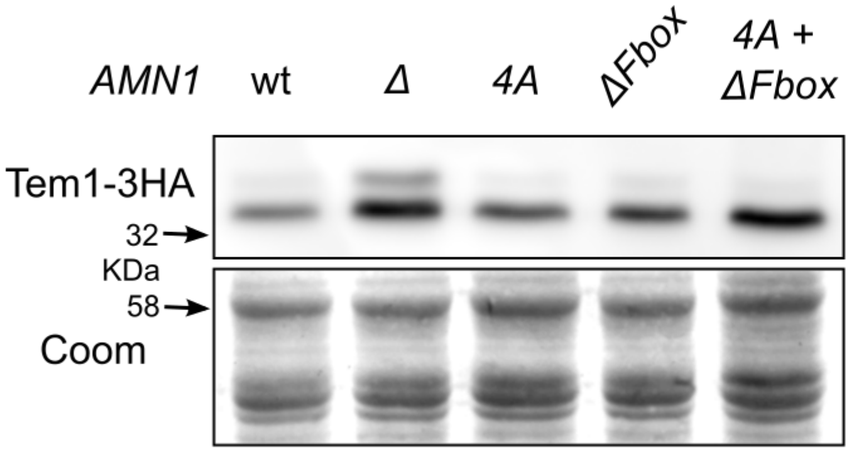

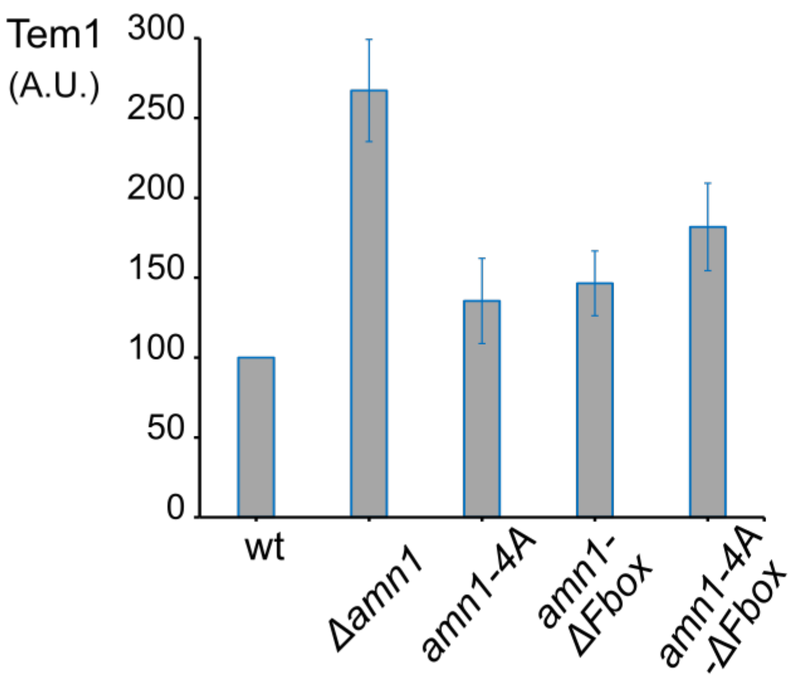

G

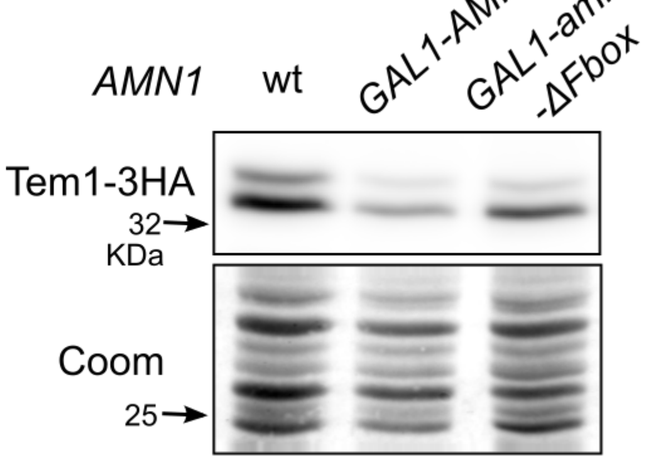

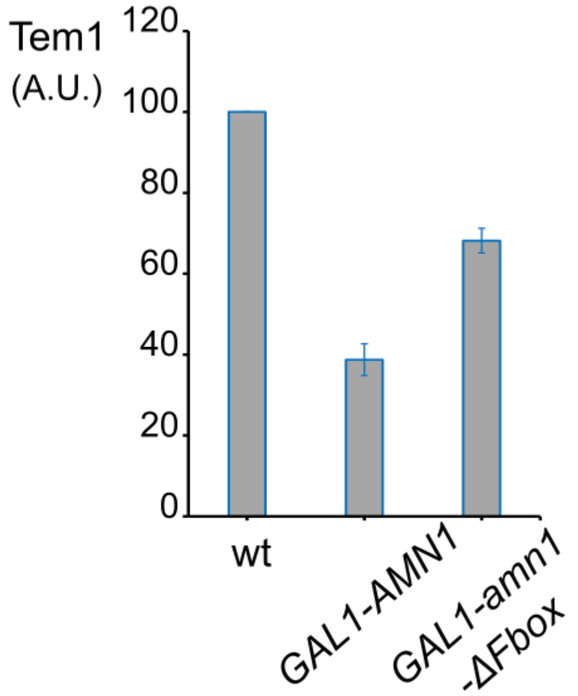

Devault and Piatti Fig. 4